JAAS

PAPER

View Article Online
View Journal | View Issue

Cite this: *J. Anal. At. Spectrom.*, 2016, **31**, 2410

Matrix effects and mass bias caused by inorganic acids on boron isotope determination by multi-collector ICP-MS

Xuefei Chen,[ab] Le Zhang,[ab] Gangjian Wei*[a] and Jinlong Ma*[a]

Received 2nd September 2016
Accepted 27th October 2016

DOI: 10.1039/c6ja00328a

www.rsc.org/jaas

The influence of inorganic acids (HCl, HNO_3, and HF) on boron isotope measurement by using multi-collector inductively coupled plasma mass spectrometry (MC-ICP-MS) has been investigated. The acid concentration is in the range of 0–0.2 M. Generally, acids can enhance B signal intensities and reduce isotopic mass bias compared to that of the same B concentration in a H_2O matrix. The signal enhancement in each acid matrix differs slightly, while B isotopic mass bias is significantly different among them, with the highest $^{11}B/^{10}B$ ratio in the HF matrix and the lowest in the HCl matrix. In HCl and HNO_3 matrices, boron isotopic mass bias reduces when the acid concentration goes up. However, such a scenario is not observed in the HF matrix. Furthermore, the $^{11}B/^{10}B$ ratio in the HF matrix is the same as that in the H_2O matrix within the studied acid concentration (up to 0.2 M). This implies that changes in mass bias and the B signal cannot be related to the same process in ICP-MS. We suggest that B signal enhancement in inorganic acids can mainly be attributed to Coulomb fission during aerosol transport towards plasma, while boron ion redistributions in the plasma caused by matrix element (*e.g.* Cl, N) ionization lead to changes in isotopic mass bias. As acids can cause considerable matrix effects and mass bias for boron, acidity match between samples and standard solutions is imperative for accurate and precise B isotope measurement by MC-ICP-MS.

Introduction

Light element boron (B) has two isotopes ^{11}B and ^{10}B, which make up approximately 80.1% and 19.9% of the total boron, respectively.[1] With a relatively large mass difference, boron isotopes experience large fractionations in nature.[2] Furthermore, the chemical and biological properties of boron make it a very promising element to study for its isotopic variations in many fields such as: (1) geochemical proxy for paleo-pH of the oceans;[3–5] (2) geochemical tracer for studying high- and low-temperature fluid-related processes;[6–8] (3) chemical weathering;[9–11] (4) tracer for anthropogenic pollution;[12,13] and (5) B behavior in higher plants.[14,15]

MC-ICP-MS has become the most common approach for boron isotope measurements in recent years,[16–25] for it is more rapid and convenient to be carried out, and possesses the ability to maintain better temporal stability. Based on this instrument, several chemical treatments have been developed for separating boron from complicated matrices (*e.g.* silicates, carbonates, and plants *etc.*).[16–25] For different chemical procedures, the final solutions involve different types of acids (*e.g.* HCl, HNO_3, or HF) or H_2O as the introduction medium for MC-ICP-MS measurements.[16–25] Introduction of inorganic acids into the isotope analyses affects the mass bias of boron in the MC-ICP-MS.[20,22,26] Measurements performed on B standard solutions with trace HCl result in ~5% reduction in mass bias.[20] Moreover, B isotopic mass bias reduces with increasing acid concentration, and this scenario is more serious for HCl than HNO_3.[22,26] Meanwhile, ^{11}B signal intensity in the HCl matrix tends to be slightly higher than that in the HNO_3 matrix.[22] Such acid effects imply that an appropriate introduction medium and acidity match between samples and standard solutions are of critical importance for accurate and precise boron isotope ratio measurements. The mechanism for this, however, is not well known yet.

Mineral acids are the most commonly used medium for introducing analytes into the ICP-MS. The type of acid and its concentration affect the analyte signal, which can be attributed to acids' effects on aerosol generation, analyte transport, or changes in excitation and ionization processes within the plasma.[27–33] For most elements, the presence of an acid matrix can lead to signal depression compared to the H_2O matrix.[27,28,34] However, using very low concentration acids could increase signals.[31] In contrast to acids' matrix effects, few studies focus on their influences on mass bias in MC-ICP-MS.[26,35] A study on Fe isotope measurement showed that HNO_3 is superior to HCl as it yielded smaller drifts of instrumental mass bias with time and better signal stability in MC-ICP-MS.[35] In addition, as

[a]State Key Laboratory of Isotope Geochemistry, Guangzhou Institute of Geochemistry, Chinese Academy of Sciences, Guangzhou, 510640, China. E-mail: gjwei@gig.ac.cn; jlma@gig.ac.cn; Fax: +86-20-85290130; Tel: +86-20-85290093; +86-20-85290116
[b]The University of Chinese Academy of Sciences, Beijing, 100039, China

outlined above, mass bias for boron isotopes is greatly affected by the type of acid and its concentration.[22,26] Given that boron is a light element and experiences relatively large mass bias (>10%) in MC-ICP-MS,[23,36] investigation of inorganic acids' effects on its behavior in the plasma may provide an isotopic perspective on mass bias and matrix effects in MC-ICP-MS.

In the present study, we adopted three generally used inorganic acids (*i.e.* HCl, HNO_3, and HF) to study their effects on boron signal intensity and mass discrimination, and also examined the distribution of B ions in the plasma of both acids (*i.e.* 0.1 M HCl and HNO_3) and the acid-free matrix (H_2O) for a better understanding of boron behaviors in MC-ICP-MS. This work may help to find out the most suitable solution medium for boron isotope measurements.

Experimental

Instrumentation

Experiments were carried out using a MC-ICP-MS (Neptune plus, Thermo Fisher Scientific) at the State Key Laboratory of Isotope Geochemistry, Guangzhou Institute of Geochemistry, Chinese Academy of Sciences. This instrument is a double focusing magnetic sector field mass spectrometer equipped with 9 Faraday cups and 9 ion counters, which enables a static measurement of m/z 10 and m/z 11 on Faraday cups. The sample was introduced into the plasma using a low-flow PFA nebulizer (self-uptake) with a nominal uptake rate of 50 μL min^{-1} and a cyclonic PFA spray chamber and a sapphire injector. Such an introduction system can tolerate HF, as trace HF is added into wash solution to reduce boron memory. The X skimmer cone and Pt sampler cone were used to enhance analytical sensitivity enabling ~50 ppb boron yielding a ^{11}B intensity of 0.8–1 V.

Typical operating conditions are listed in Table 1.

Reagents and standards

BVIII grade (for electronic production) hydrofluoric acid (49%) and ultrapure grade hydrochloric acid, added with ~0.25 g L^{-1} mannitol were sub-boiled using a Savillex DST-1000 system at a temperature <60 °C, which produced 2 ng mL^{-1} and 0.2 ng mL^{-1} boron blanks for concentrated HF and HCl, respectively. The ultrapure grade nitric acid (Fisher Scientific, Canada) in which the boron blank is below 5 ng mL^{-1} was directly used without further distillation. All the solutions were prepared using de-ionized water which was purified by using a Millipore system coupled with Q-Gard Boron that can effectively remove boron. For boron isotope measurements, a NIST SRM 951 boric acid isotopic reference material and three $\delta^{11}B$ reference materials, ERM AE120, AE121, and AE122, available from the Federal Institute for Materials Research and Testing (BAM, Germany) (*i.e.* $\delta^{11}B = -20.2 \pm 0.6\%$, $19.9 \pm 0.6\%$, $39.7 \pm 0.6\%$, respectively), were used.

Table 1 Typical operating parameters for B isotope measurement on Neptune

Parameter	Value
RF forward power	940–1100 W
Ar cooling gas flow	16 L min^{-1}
Ar auxilliary gas flow	0.9 L min^{-1}
Ar sample gas flow	~1.0 L min^{-1}
Extraction voltage	2000 V
Acceleration voltage	10 000 V
Detection system	L3, H3 Faraday cups
Nebulizer	MicroFlow PFA-50 (50 μL min^{-1})
Spray chamber	47 mm PFA spray chamber
Injector	Sapphire injector
Sampler cone	TF1001-Ni/Cu nickel
Skimmer cone	TF1008-Pt high performance skimmer cone, platinum
Instrument resolution	400 (low)
Integration time	4.194 s
Idle time	3 s

Experimental design and analytical methods

Analytical methods. The typical operating conditions for boron isotope measurement and measuring strategies are summarized in the report of Wei *et al.*[18] Before commencing the analytical session, the instrument was tuned to a robust condition in which small changes in X or Z positions of the torch or sample gas flow rate induce little fluctuation in ^{11}B signals for SRM 951. The washing process is set to three steps: 0.1 M HCl for 3 min to reduce the ^{11}B signal to 0.12–0.15 V; 0.3 M HCl + 0.1 M HF for 3 min to reduce the ^{11}B signal to ~20 mV; and finally 0.1 M HCl for 3 min to reduce it to 6–7 mV. For the HNO_3 matrix, washing solution was changed from HCl to HNO_3 with equivalent molarity. For H_2O and HF matrices, washing solution was basically the same as used for the HCl matrix, only in the last step 0.1 M HCl changed to H_2O. As transient signal shifts may occur during acid switching for either types or concentrations, it normally takes 1–2 min to return to the steady-state level. The long-term $\delta^{11}B$ of SRM 951 is 0.02 ± 0.48% ($n = 50$; 2 standard deviation, SD).

Acid effects. In order to study possible acid effects of inorganic acids, three types of inorganic acids, HCl, HNO_3, and HF, were used in this study. To compare their influences on boron signal intensity in MC-ICP-MS, we examined the ^{11}B signal intensity (40 ppb) in each acid matrix (0.1 M) and H_2O at varying carrier gas flow rates. Further, to obtain the relationship between the acid concentration and ^{11}B signal, SRM 951 solutions prepared with equivalent B content but varying acid concentrations (from 0 to 1 M) for each acid matrix were measured for their ^{11}B intensities. As for possible matrix-dependent mass discrimination of inorganic acids, we determined the B isotopic compositions of SRM 951 solutions (50 ppb) prepared with a series of acid concentration (0–0.2 M) for each acid matrix. The bracketing reference solutions were set at 0.1 M with the same acid used accordingly for the sample, with the exception that H_2O was used as the standard solution for the HF matrix. Further, to examine whether the acidity effects on B mass bias are also influenced by the B isotopic composition of analyte solution, we prepared a series of standard solutions (SRM 951, ERM-AE120–AE122) with an equivalent B concentration in a range of HCl concentrations and measured their B isotopic compositions against SRM 951 in 0.1 M HCl.

Radial and axial distribution of B in plasma. The B ion distribution profiles were obtained by moving the ICP torch horizontally between −4.02 mm and 2.92 mm across the sampler cone orifice (changed with the *X* position of the torch box) and by moving the ICP torch forward and backward between its end and the sampler cone (changed with the *Z* position of the torch box). Considering that the torch when close to the sampler cone ($Z < 1.5$ mm) may cause plasma flameout, the *Z* position variation range is set within 1.70 mm to 3.62 mm. Throughout the entire analytical session the *Y* position of the ICP torch remains unchanged and is set as −1.7 mm.

Results and discussion

Signal enhancement

Generally, boron signal enhancement is observed in an ionic matrix compared to that in H_2O, and the optimum carrier gas flow rate is the same for each solution matrix (Fig. 1a), which may be due to the low acid concentration (0.1 M) used in this study insignificantly to cause shifts in the optimum carrier gas flow rate. The magnitude of signal enhancement in HF is slightly higher than that in other acid matrices, especially at the optimum carrier gas flow rate. ^{11}B signal intensities in HCl and HNO_3 are basically identical which differs from the previous observation that the ^{11}B signal is higher in HCl than in HNO_3.[22] As for the effects of the acid concentration, in all acid matrices the ^{11}B signal rises to the highest when the acid concentration approaches 0.02 M and then remains constant with further acid concentration elevation to 0.1–0.2 M, and afterwards drops rapidly as the acid concentration increases to 1 M (Fig. 1b). This scenario is also in contrast to what has been observed by Roux *et al.*[22] that in the HCl matrix ^{11}B signal intensity increases as the acid concentration goes up (from 0.1 to 1.5 M) whereas ^{11}B signal intensity in the HNO_3 matrix seems to be indifferent to the acid concentration within the same range. The reason for these discrepancies is not quite clear, but we suggest that it may arise from different conditions of MC-ICP-MS, for the instrumental sensitivity in the study of Roux *et al.*[22] is much lower (5 V per μg g^{-1}) than that in this study (20 V per μg g^{-1}).

Nevertheless, ^{11}B signal enhancement in acid matrices compared to the water matrix is in contrast to most previous observations that analyte signal intensities (*e.g.* Ba, Al, and Mn, *etc.*) tend to decrease with increasing acid concentration.[27,28,37] However, different acid effects on the analyte signal are quite reasonable for many sources or processes, including the nature and concentration of the analyte or matrix, contribute to the ultimate analyte behaviors in the ICP-MS.[38] For instance, under robust ICP-MS conditions (high incident power and low nebulizer gas flow) signal enhancements do occur in inorganic acid matrixes.[28] Moreover, in low acid concentrations (<1% v/v) there is an increase in the analyte signal for HCl with a maximum intensity at ~0.001% v/v HCl, but little signal changes for HNO_3.[31]

When the sample matrix is changed from H_2O to inorganic acids, it would induce a great number of changes in aerosol properties, analyte and aerosol transport rate, and local plasma conditions, which all determine the signal intensity behavior.[38] Generally, the presence of an acid matrix can reduce solvent evaporation, as evaporation is more efficient for 0% acid (*i.e.* H_2O) and the more the acid concentration the less efficient it is.[27] As a consequence, with increasing acid concentration there is less water but more acid transported as aerosol into the plasma. Such changes will increase the relative liquid density of the aerosol and then lower the aerosol transport rate to the plasma, leading to the drop in the signal intensity.[27,28,33] In addition, hydrogen is also important in the plasma, because its high thermal conductivity enables the energy transfer between the bulk of the plasma and the central channel, hence promoting analyte ionization. On a molar basis, H_2O provides more H to the plasma than monoacid, indicating that in terms of hydrogen acid concentration increase may result in signal suppression.[28] In this study, however, the ^{11}B signal is enhanced rather than suppressed, suggesting that acid effects on solvent evaporation and the associated aerosol transport rate, as well as the presence of H have restricted effects on B behavior in the

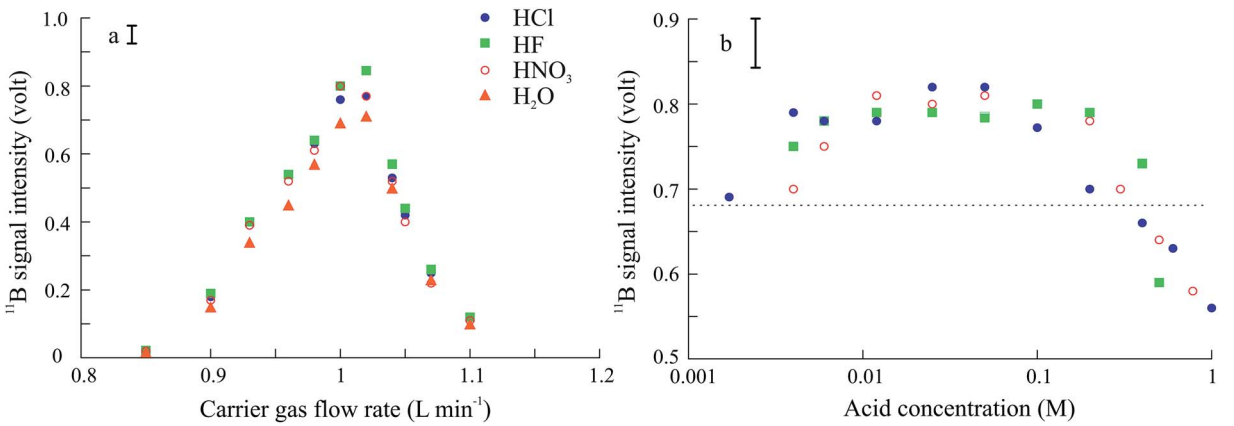

Fig. 1 Boron signal behaviors in inorganic acids and H_2O: (a) ^{11}B signal in different acids (0.1 M) and H_2O at a varying carrier gas flow rate; (b) ^{11}B signal changes with increasing acid concentration in different acid matrices. The dashed line indicates the ^{11}B signal of H_2O. All solutions contained ~40 ppb boron.

ICP-MS. It is possible that other processes (*e.g.* formation of usable droplets for the ICP) may counteract the reduction in evaporation, or that in low acid concentration the solvent evaporation rate and the solution density change slightly compared with water leading to little variation in the analyte transport rate.

In inorganic acid matrices, the tertiary drop size distribution tends to shift to lower diameters with increasing acid concentration, especially at low nebulizer gas flow rates and a low acid concentration range.[27] Aerosols produced by pneumatic nebulization are composed of droplets with a net charge, and droplets containing an ionic matrix are prone to carry a charge compared to matrix-free ones.[39] The increases of the net charge of droplets will lead to Coulomb fission during transport through the spray chamber, as the surface tension is exceeded by coulombic repulsions and then a parent droplet splits into smaller progeny droplets and releases the excess charge.[40] Such a scenario is more effective for tertiary aerosol formation. Generally, the primary aerosol drop size is hardly affected by changes in the acid concentration, whereas tertiary aerosol tends to form smaller droplets with increasing acid concentration.[27,41] Paredes *et al.*[37] found that in a low concentration inorganic acid matrix (*i.e.* below 0.38 M and 0.40 M for nitric and hydrochloric acids, respectively), finer tertiary aerosols were indeed produced by droplet fission (or Coulomb fission) with increasing acid concentration. Therefore, it is suggested that an acid matrix can facilitate the formation of more usable droplets for the ICP, and hence produce a signal enhancement compared to the H_2O matrix. Nevertheless, previous studies found that signal intensities of most analyte elements (*e.g.* Co, Ba, and Mn, and Al) tend to reduce in an acid matrix in comparison to plain water, regardless of a decreased tertiary drop size distribution.[27,37] For these studies, the analyte elements are mainly easily ionized elements (EIEs). Formation of finer droplets for plasma for these EIEs may not be as important as it is for B ionization in the ICP plasma for B is estimated to be only 58% ionized. Therefore, we suggest that droplet fission in an acid matrix contributes to B ionization in the plasma, leading to the increase of ^{11}B signal intensities in an acid matrix. As also pointed out by Paredes *et al.*,[37] droplet fission is limited; once the acid concentration reaches a certain high value, it will cause a delay in solvent evaporation and the fission decreases, and then the size of droplets remains steady. This may explain our finding that the ^{11}B signal enhancement reaches a plateau after the acid concentration increases to 0.02 M and then falls down with further increase of acid concentration (Fig. 1b). Therefore, we suggest that B signal enhancement in low concentration inorganic acids can mainly be attributed to increased droplet fission in the presence of an ionic matrix.

Mass bias variation as a function of the acid concentration

Boron, being a light element, suffers significant mass bias (>10%) in MC-ICP-MS. It has been found that mass bias for B isotopes is influenced by both the solution matrix and its concentration.[20,22,26] In nitric and hydrochloric acids, $^{11}B/^{10}B$ ratios decreased with increasing acid concentration.[17,22,26] In this study, Fig. 2 also confirms that for HNO_3 and HCl matrixes changes in the acid concentration can induce significant mass bias for boron isotopes in MC-ICP-MS. In the range of 0 to 0.2 M, the $\delta^{11}B$ value shows a descending trend as the acid concentration goes up in both the HCl and HNO_3 matrixes, while in the HF matrix the $\delta^{11}B$ value varies slightly with respect to analytical precision (Fig. 2). As can also be seen from Fig. 2, $\delta^{11}B$ values of SRM 951 in H_2O (*i.e.* 0 M HCl or HNO_3) are calculated to be higher against 0.1 M HCl than HNO_3, and all are higher than 0%, while little offset exists between $\delta^{11}B$ values

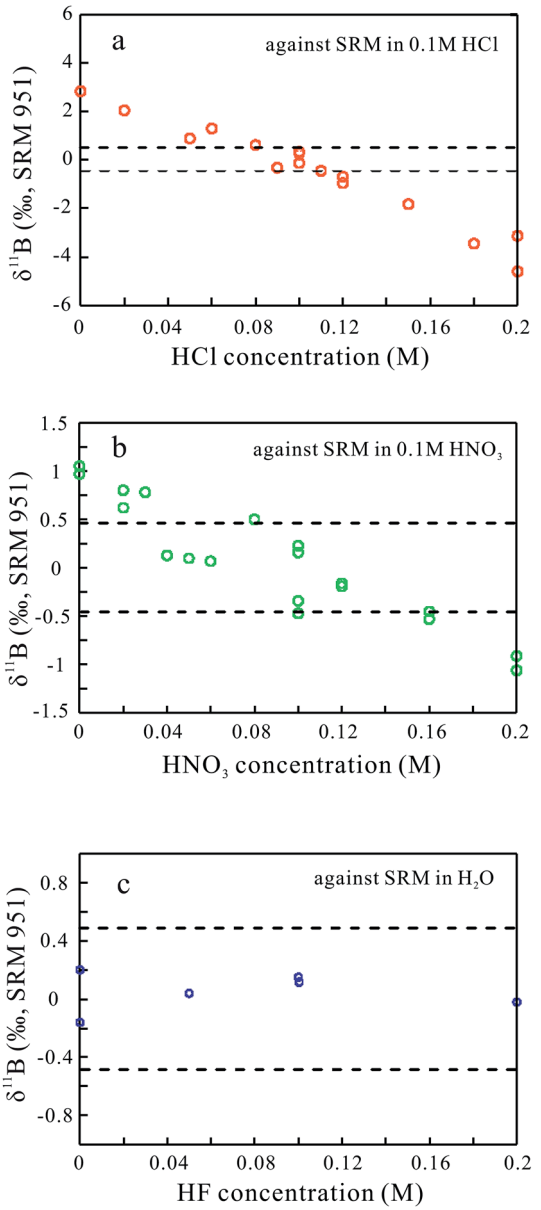

Fig. 2 Effects of the inorganic acid concentration on $\delta^{11}B$ (%) values of SRM 951: (a) HCl, (b) HNO_3, and (c) HF. All solutions contained ~50 ppb boron, and were measured against bracketing SRM 951 solution in (a) 0.1 M HCl, (b) 0.1 M HNO_3, and (c) H_2O. The interval between the two dashed lines in each diagram indicates the long-term 2 standard deviations of SRM 951 (2SD = 0.48).

of SRM 951 in H_2O and 0.1 M HF. This means that higher isotopic mass discrimination, namely higher $^{11}B/^{10}B$ ratios, tend to occur in H_2O or HF matrices, and HCl and HNO_3 matrices can be helpful to reduce boron mass bias. Furthermore, the magnitude of isotopic mass bias caused by the HCl matrix is considerably large compared to that of the HNO_3 matrix, which is consistent with the previous observations.[22,26] The considerable differences for boron isotopic fractionation indicate that changes in B mass bias and signal intensity in different acid matrices are caused by different processes in the ICP-MS, and the nature of acid itself has great impacts on the behaviors of boron isotopes in the ICP-MS. In addition, as can be seen from Fig. 3, acidity induced mass bias is hardly influenced by the B isotopic compositions of the analyte, as the deviation of each standard (*i.e.* measured values–certified values) at a certain HCl concentration is basically the same. Therefore, the calculated regression equations show similar slopes but varying intercepts. The parallel regression lines in Fig. 3 suggest that the deviations of the measured $\delta^{11}B$ caused by acidity mismatch could be corrected at the same time for the samples with different boron isotopic compositions.

Mass bias is typically generated by processes occurring both in the plasma and in the interface.[36,42] Matrix-dependent vaporization, ionization, and diffusion are all important factors affecting mass discrimination.[43] Since the parameters with respect to the sampler and the skimmer cone remain constant, we believe that the variability of mass bias observed in this study is due mainly to the processes happening in the plasma. As outlined above, vaporization changes in acid matrices (0.1 M) are relatively small compared with H_2O. Therefore, matrix-dependent ionization and/or diffusion appear to be the dominant process affecting the B behavior in the plasma. It is noted that the magnitude of mass bias for B caused by different acids follows the order, HCl < HNO_3 < HF, which is identical to the order of first ionization potential of the three component elements, *i.e.* Cl < N < F.[44] This suggests that matrix elements affect analyte ionization or diffusion, and thus the B ion distribution in the ICP.

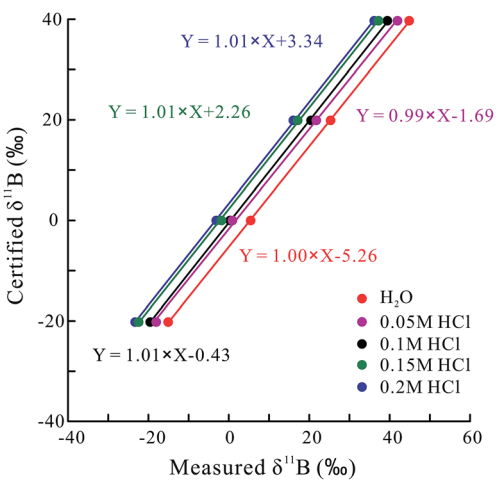

Fig. 3 Effects of the HCl concentration on standard solutions with different $\delta^{11}B$ (%) values. All solutions contain 50 ppb boron, and were measured bracketed by SRM 951 solution in 0.1 M HCl. The certified $\delta^{11}B$ (%) values of different standard solutions are 39.7 ± 0.6% for ERM-AE122, 19.9 ± 0.6% for ERM-AE121, 0% for SRM 951, and −20.2 ± 0.6% for ERM-AE120, respectively.

The spatial profiles of B ion and $^{11}B/^{10}B$ ratio distributions in the plasma

Changes in B intensities and mass bias in different inorganic acids may reflect variations of B ion distributions in the plasma. Fig. 4 presents the spatial distributions of the B ion, $^{11}B/^{10}B$ ratios, and the instrumental uncertainties in the plasma of different matrices, *i.e.* H_2O, 0.1 M HNO_3, and 0.1 M HCl.

Effect of the torch radial position. The ^{11}B intensity and $^{11}B/^{10}B$ ratio profiles all exhibit a symmetric distribution in the radial direction. ^{11}B intensity reaches the highest in the center of the plasma and can decrease to approximately 30% of the maximum at 0.6 mm off-axis, while $^{11}B/^{10}B$ ratios display an opposite variation trend with the lowest values occurring with the maximum ^{11}B intensity and highest values occurring with the minimum ^{11}B intensity (Fig. 4). This trend is similar to the distribution profiles of other elements and their isotopic ratios in the plasma (*e.g.* Pb[43] and Cu[36]), and is attributed to the mass dependent radial diffusion that lighter isotopes have greater dispersal rates.[29,45] It seems that the analytical precision for $^{11}B/^{10}B$ ratios are indifferent to the changes of the *X* position of the torch along a given *Z*-value section. Only when the torch sites are at the extreme off-axis positions will the instrumental uncertainties increase dramatically.

Effects of the sampling depth. The ^{11}B intensity profiles also exhibit a symmetric distribution in the axial direction (Fig. 4), but the symmetric profiles are not fully revealed for water and nitric acid matrixes because of the limited range of the torch *Z* position. In contrast, axial $^{11}B/^{10}B$ ratio profiles present an asymmetric distribution with a steep increase in the $^{11}B/^{10}B$ ratio with increasing sampling depth (Fig. 4). Such isotope ratio variations can be explained using the zone model that lighter isotopes reach maximum density closer to the end of the torch than heavier isotopes do.[29] Therefore, with increasing sampling depth, more ^{11}B ions enter the sampler cone resulting in a higher $^{11}B/^{10}B$ ratio. Meanwhile, the analytical precision also augments the increasing $^{11}B/^{10}B$ ratio, suggesting that mass bias caused by the sampling depth impacts the precision of $^{11}B/^{10}B$ ratio measurements. The different responses of instrumental uncertainties to changes in the torch radial position and sampling depth indicate that the sampling depth exerts a greater influence on mass discrimination for B isotopes and hence the analytical precision. Comparing the analytical precision with ^{11}B signal intensity and $^{11}B/^{10}B$ ratios, it is found that both parameters are important factors controlling the analytical precision, but with the latter's influence more pronounced (Table 2). This may explain why the spatial profile of analytical precision in Fig. 4 looks like the profile of the $^{11}B/^{10}B$ ratio rather than that of B intensity.

Generally, B ion distributions in the three matrices are quite different. B intensities show irregular distribution in the plasma of the water matrix, while B ions distribute elliptically and

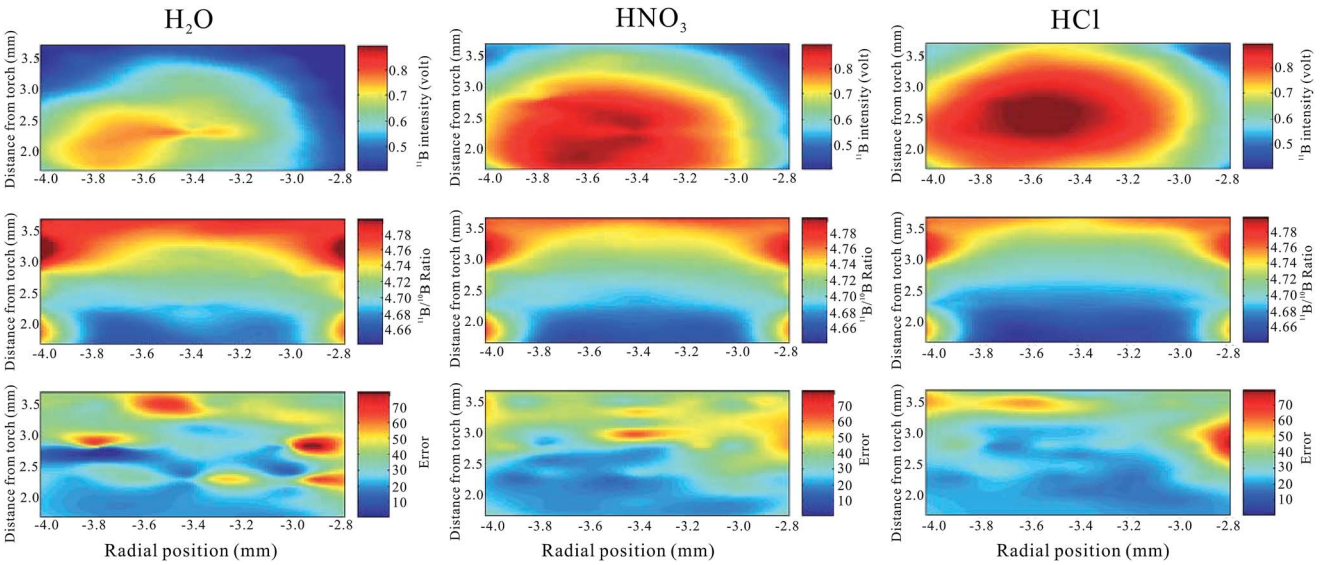

Fig. 4 Distributions of boron ions (upper panel), $^{11}B/^{10}B$ ratios (middle panel) and analytical precision (lower panel) in the plasma of different matrices.

Table 2 Correlations between analytical precision and ^{11}B signal intensity, and $^{11}B/^{10}B$[a]

	^{11}B intensity *vs.* analytical precision	$^{11}B/^{10}B$ *vs.* analytical precision
H_2O	0.51	0.52
HNO_3	0.61	0.76
HCl	0.61	0.68

[a] The correlation analysis is based on the data for Fig. 4; for all the calculation $n = 120$, $p < 0.05$.

symmetrically for inorganic acids. The ion cloud in the plasma is theoretically regular and circular, but instrumental instability may compromise the results. This suggests that signal stability in acids is better than that in H_2O. The spatial profiles of B ions also expand in inorganic acid matrices compared to that in the water matrix and the maximum ^{11}B intensity distribution in the center position of the plasma extends as well. Such changes are in contrast to the observation under the dry plasma conditions wherein adding N_2 to the plasma not only elongated the spatial profile of the B ion distribution, but also decreased the ^{11}B intensity in the center position in the ion contour.[46] This implies that addition of N_2 does not promote B ionization so that total B ions in the plasma changes little and hence the expansion of the B ion distribution results in decreased intensity.[46] With respect to wet plasma, the concurrent increase in ^{11}B intensity and its distribution area indicate that inorganic acids can promote B ionization in the plasma. This is consistent with the suggestion that more usable droplets transported into the ICP in the presence of an acid matrix promote the analyte ionization and enhance the signal. Nevertheless, for different acid matrices there also exist several differences in the spatial distribution of B ions: (1) the ion contour in the HCl matrix is more regular, (2) the high ^{11}B intensity area (dark red) is relatively larger than that in the HNO_3 matrix, and (3) the center of the maximum ^{11}B intensity zone for the HCl matrix is slightly closer toward the sampler cone than that for the HNO_3 matrix.

The distributions of $^{11}B/^{10}B$ ratios in the plasma also expand in acid matrixes as B ions redistribute (Fig. 4). The mass bias for B in the HCl matrix is decreased, as the lower $^{11}B/^{10}B$ ratio (dark blue) area enlarges (Fig. 4). The enhanced B intensity and decreased mass discrimination for B isotopes in inorganic acids indicate that acid matrices can provide robust conditions for B isotope measurement, and therefore lower instrumental uncertainties are much easier to obtain when tuning the instrument in acid matrixes (Fig. 4).

Influence of different acid matrices in the plasma

The varying degree of mass bias for B isotopes caused by different acid matrices (Fig. 2) and different B ion distributions in the plasma (Fig. 4) all point to the fact that the nature of the solution matrix plays an important role in boron isotope measurement by MC-ICP-MS. Given that the acidity (or pH) is the same for each acid matrix that is used in this study, the remarkable differences among them are the component elements and hence the background ions present in the ICP of each acid matrix (Table 3). Different matrix elements in the ICP may act to cause different effects on B ionizations for N, Cl, and F possess diverse first ionization potential. Ionization of matrix elements in the plasma can promote the ionization of the analyte element and hence elevate the signal intensity.[43] According to Houk's[44] calculation, however, the hardly ionized elements (*e.g.* H, N, O, Cl, F, *etc.*) can only be slightly ionized in the plasma. In particular, F should be barely ionized in the plasma (F is estimated to be only 0.0009% ionized in the plasma). H, N, and O should be 0.1% ionized and Cl should be 0.9% ionized in the plasma.[44] Therefore, ionization of matrix

Table 3 Background ions observed in different matrices

Solution matrix	Ions
Major background ions	
H_2O[a]	H^+
	O^+
	H_2O^+
	Ar^+
	ArH^+
HNO_3	N^+
	ArN^+
HCl	Cl^+
	$ArCl^+$
	HCl^+
HF	ArF^+
	HF^+
Additional background ions	
	O_2^+
	N_2^+
	Ar_2^+
	ArO^+
	NO^+

[a] Note that ions ionized in the H_2O matrix also exist in inorganic acid matrices.

elements in different acid matrices may contribute little to the enhancement of the B signal in Fig. 1. Nevertheless, once the matrix elements start to ionize they can release electrons and promote analyte ionization,[43] which may explain the discrepancy of B ion distributions in the plasma of different acid matrices. Cl is relatively easier to be ionized compared to N and O, and therefore the B ion cloud in the HCl matrix shows higher density and better regularity than HNO_3 and H_2O matrices. Moreover, acidity effects are more pronounced in HCl than in HCO_3 for which the $^{11}B/^{10}B$ ratios reduce dramatically with increasing HCl concentration. This scenario suggests that increase of the Cl concentration would to some extent boost the ionization of B and the mass dependent diffusion, hereby expanding the maximum ^{11}B signal and minimum $^{11}B/^{10}B$ ratio region. With respect to the HNO_3 matrix, its acidity effects are relatively weak compared to HCl, but acidity mismatch (>0.1 M) can also cause ~1% mass bias for boron isotopes. Compared with H_2O, the HNO_3 matrix provides more N and O to the plasma on a molar basis, hereby promoting the ionization of B. Because the ionization capability of N and O is weak (0.1% ionized) the mass bias caused by HNO_3 is less serious than HCl. For HF, as F is hardly ionized in the plasma it has little effects on the B ionization and B ion distribution in the plasma. As a consequence, due to the diverse nature of component elements the matrix effects and mass bias caused by different acids in the MC-ICP-MS are different.

Although B signal stability in HCl is better and its ion distribution is larger and more regular than that in HNO_3, the greater matrix effects caused by Cl suggest that when using the HCl matrix for boron isotope measurements by MC-ICP-MS, acidity match between samples and bracketing standard should be rigorous, otherwise a minute acidity mismatch (>0.02 M) can cause significant mass bias (beyond the analytical precision). In the HNO_3 matrix, the tolerance of acidity mismatch (~0.06 M) is better than that in the HCl matrix (~0.02 M), whereas for the HF matrix, its acidity effects cause little mass discrimination for B isotopes within 0.2 M (Fig. 2).

Conclusion

Solution matrixes have great effects on boron isotope measurement by MC-ICP-MS. Ionic matrixes like inorganic acids promote Coulomb fission during droplets transport through the spray chamber, promoting the formation of more usable droplets for the ICP and hence enhancing the signal intensity of boron. In addition, the presence of different acid matrices changes the boron ionization environment in the plasma which in turn changes the distribution of the boron ion and isotopes in the plasma and as a result also changes the extent of mass bias. The effect of a specific acid matrix depends on the first ionization potential of the component elements.

The results of this study underline the importance of selecting an appropriate acid matrix as the introduction medium, as well as acidity match between samples and standards for boron isotope measurement by MC-ICP-MS. Although in the HF matrix the ^{11}B signal can achieve higher intensity and acid match is less critically required, the hazardous nature of HF suggests that caution should be exercised when using it as an introduction medium. Considering the similar ^{11}B signal in HCl and HNO_3 but less rigorous acid match requirement in HNO_3, we recommend HNO_3 to be used in boron isotope measurements by MC-ICP-MS.

Acknowledgements

We would like to thank Ying Liu for her help on this work. This research was funded by the National Natural Sciences Foundation of China (41325012) and the National Key Research and Development Program of China (No. 2016YFA0601204) and the GIG-CAS 135 project (135PY201605). This is contribution No. IS-2310 from GIGCAS.

References

1 J. Hoefs, *Stable Isotope Geochemistry*, Springer-Verlag, Berlin, Heidelberg, 6th edn, 2009, p. 285.
2 S. Barth, *Geol. Rundsch.*, 1993, **82**, 640–651.
3 A. J. Spivack, C.-F. You and H. J. Smith, *Nature*, 1993, **363**, 149–151.
4 C. Pelejero, E. Calvo, M. T. McCulloch, J. F. Marshall, M. K. Gagan, J. M. Lough and B. N. Opdyke, *Science*, 2005, **309**, 2204–2207.
5 G. J. Wei, M. T. McCulloch, G. Mortimer, W. F. Deng and L. H. Xie, *Geochim. Cosmochim. Acta*, 2009, **73**, 2332–2346.
6 H. J. Smith, A. J. Spivack, H. Staudigel and S. R. Hart, *Chem. Geol.*, 1995, **126**, 119–135.
7 C. F. You, A. J. Spivack, J. H. Smith and J. M. Gieskes, *Geology*, 1993, **21**, 207–210.

8 E. Cannaò, S. Agostini, M. Scambelluri, S. Tonarini and M. Godard, *Geochim. Cosmochim. Acta*, 2015, **163**, 80–100.
9 E. Lemarchand, J. Schott and J. Gaillardet, *Geochim. Cosmochim. Acta*, 2005, **69**, 3519–3533.
10 E. Lemarchand, J. Schott and J. Gaillardet, *Earth Planet. Sci. Lett.*, 2007, **260**, 277–296.
11 A. Voinot, D. Lemarchand, C. Collignon, M. Granet, F. Chabaux and M. P. Turpault, *Geochim. Cosmochim. Acta*, 2013, **117**, 144–160.
12 W. H. Schlesinger and A. Vengosh, *Global Biogeochem. Cycles*, 2016, **230**, 19–230.
13 G. R. Davidson and R. L. Bassett, *Environ. Sci. Technol.*, 1993, **27**, 172–176.
14 J. He, J. Cui, D. Zhu, W. Zhou, S. Liao and M. Geng, *J. Plant Nutr. Soil Sci.*, 2015, **178**, 935–943.
15 M. E. Wieser, S. S. Iyer, H. R. Krouse and M. I. Cantagallo, *Appl. Geochem.*, 2001, **16**, 317–322.
16 G. Foster, *Earth Planet. Sci. Lett.*, 2008, **271**, 254–266.
17 P. Louvat, J. Bouchez and G. Paris, *Geostand. Geoanal. Res.*, 2011, **35**, 75–88.
18 G. J. Wei, J. X. Wei, Y. Liu, T. Ke, Z. Y. Ren, J. L. Ma and Y. G. Xu, *J. Anal. At. Spectrom.*, 2013, **28**, 606–612.
19 M. T. McCulloch, M. Holcomb, K. Rankenburg and J. A. Trotter, *Rapid Commun. Mass Spectrom.*, 2014, **28**, 2704–2712.
20 J. K. Aggarwal, D. Sheppard, K. Mezger and E. Pernicka, *Chem. Geol.*, 2003, **199**, 331–342.
21 K. Van Hoecke, V. Devulder, P. Claeys, P. Degryse and F. Vanhaecke, *J. Anal. At. Spectrom.*, 2014, **29**, 1819–1826.
22 P. Roux, D. Lemarchand, H. J. Hughes and M.-P. Turpault, *Geostand. Geoanal. Res.*, 2015, **39**, 453–466.
23 C. Guerrot, R. Millot, M. Robert and P. Négrel, *Geostand. Geoanal. Res.*, 2011, **35**, 275–284.
24 B.-S. Wang, C.-F. You, K.-F. Huang, S.-F. Wu, S. K. Aggarwal, C.-H. Chung and P.-Y. Lin, *Talanta*, 2010, **82**, 1378–1384.
25 S. Misra, R. Owen, J. Kerr, M. Greaves and H. Elderfield, *Geochim. Cosmochim. Acta*, 2014, **140**, 531–552.
26 M. Holcomb, K. Rankenburg and M. McCulloch, in *Principles and Practice of Analytical Techniques in Geosciences*, The Royal Society of Chemistry, 2015, pp. 251–270.
27 I. I. Stewart and J. W. Olesik, *J. Anal. At. Spectrom.*, 1998, **13**, 1249–1256.
28 I. I. Stewart and J. W. Olesik, *J. Anal. At. Spectrom.*, 1998, **13**, 1313–1320.
29 F. Vanhaecke, R. Dams and C. Vandecasteele, *J. Anal. At. Spectrom.*, 1993, **8**, 433–438.
30 S. H. Tan and G. Horlick, *J. Anal. At. Spectrom.*, 1987, **2**, 745–763.
31 M. Marichy, M. Mermet and J. M. Mermet, *Spectrochim. Acta, Part B*, 1990, **45**, 1195–1201.
32 A. Canals, V. Hernandis, J. L. Todolí and R. F. Browner, *Spectrochim. Acta, Part B*, 1995, **50**, 305–321.
33 A. Fernandez, M. Murillo, N. Carrion and J.-M. Mermet, *J. Anal. At. Spectrom.*, 1994, **9**, 217–221.
34 S. S. Q. Hee, T. J. Macdonald and J. R. Boyle, *Anal. Chem.*, 1985, **57**, 1242–1252.
35 R. Schoenberg and F. von Blanckenburg, *Int. J. Mass Spectrom.*, 2005, **242**, 257–272.
36 H. Andren, I. Rodushkin, A. Stenberg, D. Malinovsky and D. C. Baxter, *J. Anal. At. Spectrom.*, 2004, **19**, 1217–1224.
37 E. Paredes, S. E. Maestre and J. L. Todolí, *Spectrochim. Acta, Part B*, 2006, **61**, 326–339.
38 C. Agatemor and D. Beauchemin, *Anal. Chim. Acta*, 2011, **706**, 66–83.
39 Q. Xu, G. Mattu and G. R. Agnes, *Appl. Spectrosc.*, 1999, **53**, 965–973.
40 J. Q. Xu, D. Balik and G. R. Agnes, *J. Anal. At. Spectrom.*, 2001, **16**, 715–723.
41 J.-l. Todoli, J.-m. Mermet, A. Canals and V. Hernandis, *J. Anal. At. Spectrom.*, 1998, **13**, 55–62.
42 G. H. Fontaine, B. Hattendorf, B. Bourdon and D. Gunther, *J. Anal. At. Spectrom.*, 2009, **24**, 637–648.
43 J. Barling and D. Weis, *J. Anal. At. Spectrom.*, 2012, **27**, 653–662.
44 R. S. Houk, *Anal. Chem.*, 1986, **58**, 97A–105A.
45 I. I. Stewart and J. W. Olesik, *J. Am. Soc. Mass Spectrom.*, 1999, **10**, 159–174.
46 L. Lin, Z. Hu, L. Yang, W. Zhang, Y. Liu, S. Gao and S. Hu, *Chem. Geol.*, 2014, **386**, 22–30.